




# Alternating bio-based pyridinic copolymers modified with hydrophilic and hydrophobic spacers as sorbents of aromatic pollutants

Ibtissem Jalia<sup>1</sup> | Taha Chabbah<sup>1,2</sup>  | Saber Chatti<sup>1</sup>  | Frédéric Schiets<sup>3</sup> | Hervé Casabianca<sup>3</sup> | Catherine Marestin<sup>4</sup> | Régis Mercier<sup>4</sup> | Steffen M. Weidner<sup>5</sup> | Hans R. Kricheldorf<sup>6</sup> | Abdelhamid Errachid<sup>3</sup> | Emmanuelle Vulliet<sup>3</sup> | Mohamed Hammami<sup>1</sup> | Nicole Jaffrezic-Renault<sup>3</sup> 

<sup>1</sup>National Institute of Research and Physicochemical Analysis (INRAP), Biotechnopole of Sidi Thabet, Ariana, Tunisia

<sup>2</sup>Faculty of Sciences, University of Tunis El Manar, Tunis, Tunisia

<sup>3</sup>Institute of Analytical Sciences, University of Lyon, Villeurbanne, France

<sup>4</sup>Institute of Polymer Materials, University of Lyon, Villeurbanne, France

<sup>5</sup>BAM, Federal Institute of Material Research and Testing, Berlin, Germany

<sup>6</sup>Institut für Technische und Makromolekulare Chemie, Hamburg, Germany

## Correspondence

Nicole Jaffrezic-Renault, University of Lyon, Institute of Analytical Sciences, UMR 5280, 5 Rue de la Doua, 69100 Villeurbanne, France. Email: nicole.jaffrezic@univ-lyon1.fr

## Funding information

We would like to acknowledge the French Embassy, Campus France in Tunisia (Dr. Pierre Durand De Ramefort) and of the High Ministry of Education and Research in Tunisia for the financial support of the POLYAM research project. The research leading to these results has received funding from the European Union Horizon 2020 (TUNTWIN) research and innovation program under grant agreement n° 952306.

## Abstract

The main objective of this work was to design new advanced sorbent phases, alternating copolymers, derived from isosorbide and 2,6-difluoropyridine, to be used for the removal of aromatic organic pollutants present in water at low concentrations. Six different monomers, dianhydrohexitols isomers and bisphenol derivatives, were synthesized in order to make it possible to study their hydrophilic and hydrophobic effect on the sorption efficiency of the resulting polymeric phases. Before this study, we have confirmed the chemical structures, molecular weights, and thermal properties of the obtained polymeric phases. Sorption results show a higher adsorption efficiency of P6 co-poly(ether-pyridine) based on bisphenol substituted with pyridine units, for all tested pollutants, hydrophobic and hydrophilic ones, due to its less compact structure. Two aromatic organic pollutants, *p*-hydroxybenzoic acid and toluic acid, were selected as sorbates to study the adsorption characteristic, kinetics and isotherms of the co-poly(ether pyridine) P6. Langmuir model led to a better fitting of the sorption isotherms; the sorption of toluic acid is easier than that of *p*-hydroxybenzoic acid. Comparing 1/*n* values for benzoic acid was two times lower for P6 compared to that for biochar and for cross-linked methacrylate resin, showing a higher efficiency.

## KEYWORDS

alternating co-poly(ether pyridine)s, aromatic organic compounds, biosourced isosorbide, sorption isotherm, sorption mechanism

## 1 | INTRODUCTION

Benzene derivatives are the most important organic pollutants.<sup>1</sup> Some of these compounds are abundantly occurring in nature, extracted from plants or produced by the degradation of animals, others are synthesized by humans and are often used as herbicides, pesticides, drugs, disinfectants, or food additives.<sup>2</sup> They are often found in water

bodies due to the discharge of polluted wastewater from domestic, industrial, and agricultural activities.<sup>3</sup>

Combining properties of high toxicity, poor degradability, and high reactivity, benzene derivative compounds present in water have high tendencies of interacting with other components of the aquatic environment,<sup>4</sup> which can result in significant impacts on human health and safety. Indeed, exposure to benzene derivative compounds may

affect the endocrine system of humans and animals, which leads to the development of liver cancer,<sup>5</sup> kidney damage,<sup>6</sup> anemia skin,<sup>7</sup> and systemic poisoning.<sup>8</sup> Therefore, these chemical compounds are considered to be the major hazardous wastes and have been enlisted by European Union and U.S Environmental Protection Agency (USEPA).<sup>9</sup> On the other hand, because of the complexity of these compounds and their presence at low concentrations, which does not exclude their toxicity, their detection, and analysis remains difficult.<sup>10</sup>

Furthermore, the elimination of these pollutants from wastewater constitutes a major challenge. Therefore, a number of technologies have been employed to remove the benzene derivatives from wastewater, such as membrane filtration,<sup>11</sup> advanced oxidation,<sup>12</sup> ozonation,<sup>13</sup> photocatalytic degradation,<sup>14</sup> electrochemical degradation,<sup>15</sup> phytoremediation,<sup>16</sup> extraction method,<sup>17</sup> biological methods,<sup>18</sup> reverse osmosis,<sup>19</sup> and adsorption.<sup>20</sup> Some of these methods and techniques present high-removal efficiency. Nevertheless, the adsorption process remains the most widely used treatment among them. In fact, it is used for the removal of a wide variety of chemical compounds and heavy metals from wastewaters; it consumes less energy, it does not involve solvent release and the adsorbent is recyclable after desorption. To eliminate benzene derivatives compounds from aqueous systems a broad range of adsorbents have been used, including activated carbon,<sup>21</sup> silica gel,<sup>22</sup> clays,<sup>23</sup> zeolite,<sup>24</sup> metal organic framework-based materials.<sup>25</sup> Recently, several polymer adsorbents have been developed such as poly(styrenesulfonate),<sup>26</sup> cyclodextrin,<sup>27</sup> hyper-crosslinked polymers,<sup>28</sup> conjugated microporous polymers (CMPs),<sup>29</sup> styrene-divinyl benzene copolymer<sup>30</sup> and polypyrrole.<sup>31</sup> These polymeric materials present a desirable pore size distribution, large surface area, hydrolytic stability, and ability of regeneration under mild conditions, which is very important for contaminant removal. In spite of all these advantages, some aspects that may compromise the efficiency of the process must be taken into account. Among the most critical criteria, these polymeric adsorbents are not able to simultaneously remove several organic contaminants with various chemical structures present in water at low concentrations (<0.1 mmol/L) and in particular the removal of hydrophilic pollutants.

Recently, it has been shown that the development of biopolymers derived from Glux,<sup>32</sup> furan derivatives<sup>33</sup> and sugar isomers of 1,4:3,6-dianhydrohexitol (isosorbide),<sup>34</sup> are an attractive and unavoidable alternative to replace monomers derived from petrochemicals. Indeed, the latter offers a good capacity to remove a wide variety of contaminants with diverse chemical structures and different polarity at low concentrations (25  $\mu\text{mol/L}$ ).<sup>35</sup> With this in mind, the main objective of this study is the elaboration of a new adsorbent phase based on a natural bio-product in order to remove nine pollutants of various hydrophobicity. In fact, the challenge consists in the synthesis and characterization of a new partially biosourced synthon from the combination of isosorbide and pyridine that can participate in the design of six new co-poly(ether-pyridine)s in order to develop new adsorbent phases based on isosorbide with different structures. The integration of isosorbide into synthon can generate attractive hydrophilicity, wettability, superior rigidity, high-thermal property and biodegradability, as well as nontoxicity.<sup>36</sup> Lately, homopolymers containing a pyridine structure substituted with a basic character

motif have shown particular interest as potential adsorbents for micropollutants. This is particularly due to the existence of a polarized bond, which improves the solubility of the final products, through increased dipole-dipole interaction of the polymer-solvent system<sup>37</sup> as well as their chemical stability and nucleophilicity.

Inspired by the previous work of Chatti et al.,<sup>38</sup> six series of polymers were prepared from the new synthons: Family A—isomanide, isoidide, isosorbide (commercial monomers from biomass) and Family B—bisphenol A, bisphenol S (commercial monomers from petrochemical) and pyridine-modified bisphenol. In fact, the family A was chosen in order to study the effect of the isomers of isosorbide in sorption efficiency. In the family B, the bridge (dimethyl, sulfone, and methylpyridine) present between the two-benzene groups distinguishes the bisphenols. This difference of chemical structures makes it possible to obtain polymers with different structures that will present different sorption efficiency. Nine benzene derivatives compounds (toluic acid, anisic acid, benzoic acid, ferulic acid 4-chlorobenzoic, caffeic acid eugenol, and anethole) with different polarity, were selected as model contaminants to evaluate the sorption performance of the new partially biosourced poly(etherpyridine)s. Each synthesized polymer was fully characterized using NMR spectroscopy, thermal and viscosimetric methods. After the structural characterization and the thermal analysis, the sorption process was conducted in batch experiments under varying operation conditions. This work is expected to provide new insight for the conception and application of advanced adsorbents in the simultaneous and recyclable removal of organic pollutants.

## 2 | MATERIALS AND METHODS

### 2.1 | Reagents and standards

Isosorbide (**1**) was purchased from Sigma Aldrich and recrystallized from acetone, then dried over  $\text{P}_4\text{O}_{10}$  in a desiccator. Isomannide (**4**) and isoidide (**5**) were purchased from the Roquette-Frères company (Lestrem, France) and dried over  $\text{P}_4\text{O}_{10}$  in vacuum. Bisphenol A (**6**) and Bisphenol S (**7**) were purchased from Sigma Aldrich and were purified by crystallization. 4-Acetylpyridine (98%) and mercaptoacetic acid were purchased from Acros Organics. Phenol (analytical grade) was purchased from Merck. The targeted pollutants: caffeic acid (95%), 4-hydroxybenzoic acid (99%), ferulic acid (98%), benzoic acid (99.5%), eugenol (99%), p-anisic acid (98%), p-toluic acid (98%), p-chlorobenzoic acid (99%), and t-anethole (99%), were all purchased from Sigma Aldrich. Their structures and log  $p$  values are presented in Figure 1. All other chemicals: 2,6-difluoropyridine (99%), dimethylformamide (DMF, 99%), ethyl acetate, petroleum ether, anhydrous potassium carbonate ( $\text{K}_2\text{CO}_3$ ), NaCl,  $\text{Na}_2\text{SO}_4$ , and sulfuric acid (95%) were commercially available and used as received.

### 2.2 | Polymer synthesis

The generic synthetic routes for the synthesis of six new co-poly(ether-pyridine)s are presented in Figure 2. The synthesis of the different monomers is detailed in this part.

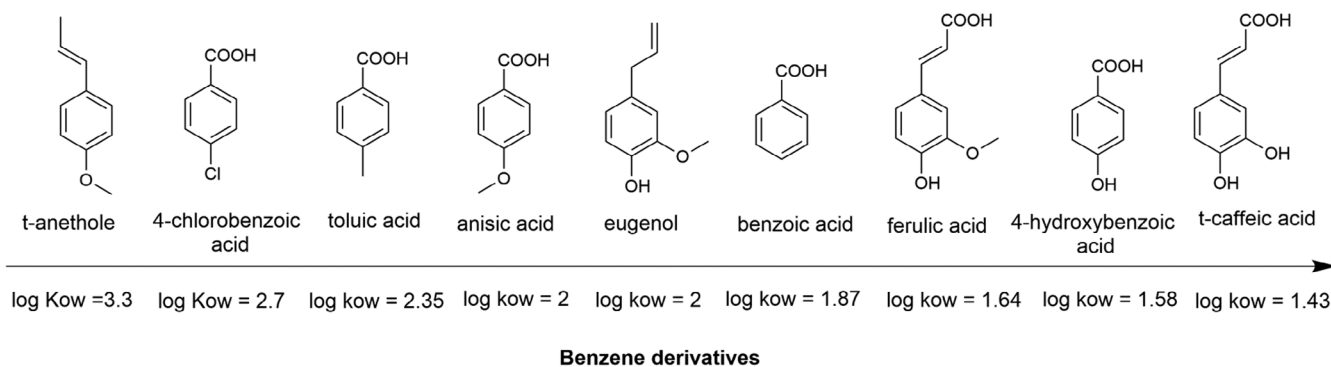


**FIGURE 1** Chemical structures and log Kow values of the targeted benzene derivative pollutants

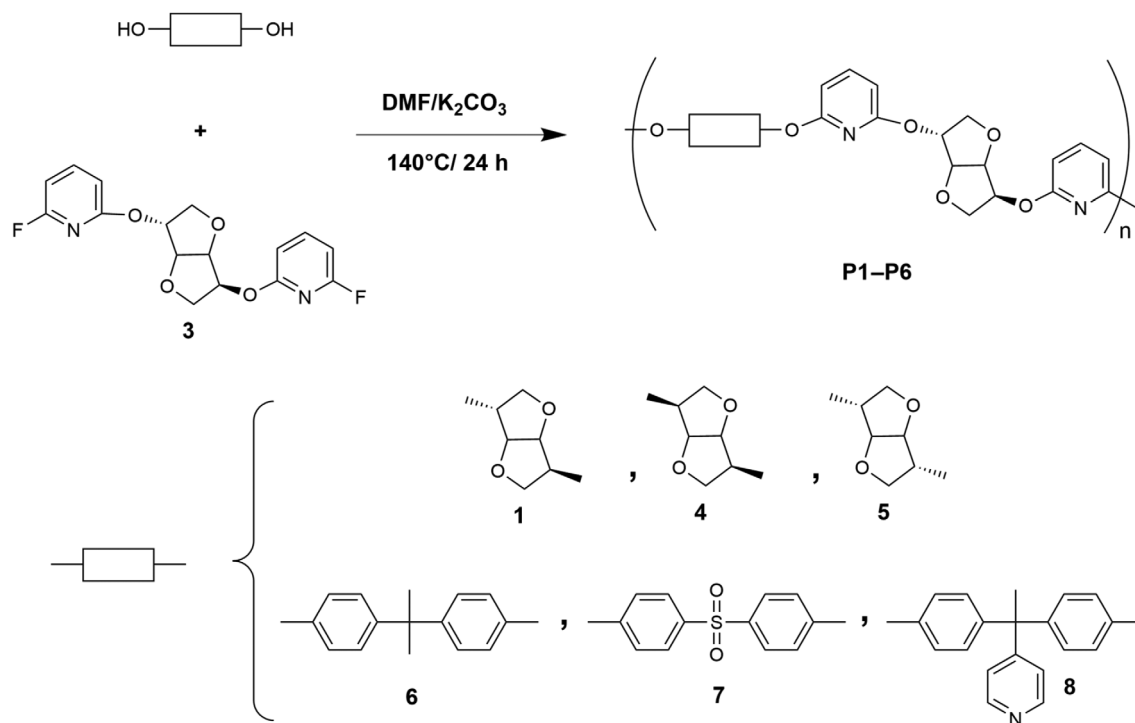


**FIGURE 2** Synthetic routes of the poly(ether-pyridine)s polymers P1–P6 (P1: (1)/(3), P2: (4)/(3), P3: (5)/(3), P4: (6)/(3), P5: (7)/(3), P6: (8)/(3)). Isosorbide (1), 2,6-difluoropyridine (2), bio-based difluoro monomer (3), isomannide (4), isoidide (5), bisphenol A (6), bisphenol S (7), bisphenol: 4,4'-(1-[pyridin-4-yl]ethane-1,1-diyl)diphenol (8)

### 2.2.1 | Synthesis of the monomer (3, type A-B-A)

(Figure 3) In a 100 ml tricol flask, 1.4616 g of isosorbide (1) was added (10 mmol) to 20 ml DMF, the solution was magnetically stirred until the isosorbide dissolved, then 500 mg of NaH was added slowly. After 20 min, a solution of 25 mmol of 2,6-difluoropyridine (2) in 10 ml DMF was added drop by drop with a dropping funnel. Then the reaction was heated to 60–70°C for 24 h and then the temperature was increased to 80°C (transparent staining) for 24 h. The mixture was then extracted with ethyl acetate and water (three times), the organic layer was dried over MgSO<sub>4</sub>. The solvent was evaporated using a rotary evaporator. To separate the monomer type B-A (3'), the monomer type A-B (3'') and the monomer type A-B-A (3), a silica gel

chromatography column with a mixture of petroleum ether and ethyl acetate (9:1) as eluent were used to obtain, after evaporation, the novel bio-based difluoro monomer (3), a yellow viscous liquid (yield = 47%).

### 2.2.2 | Synthesis of the pyridine-modified bisphenol: 4,4'-(1-[pyridin-4-yl]ethane-1,1-diyl)diphenol (8)

(Figure 4) Into a three round bottom flask equipped with a magnetic stirrer, a potassium hydroxide trap and N<sub>2</sub> inlet, were added 4-acetylpyridine (30.0 g, 243 mmol), phenol (100 g, 1.06 mol), and

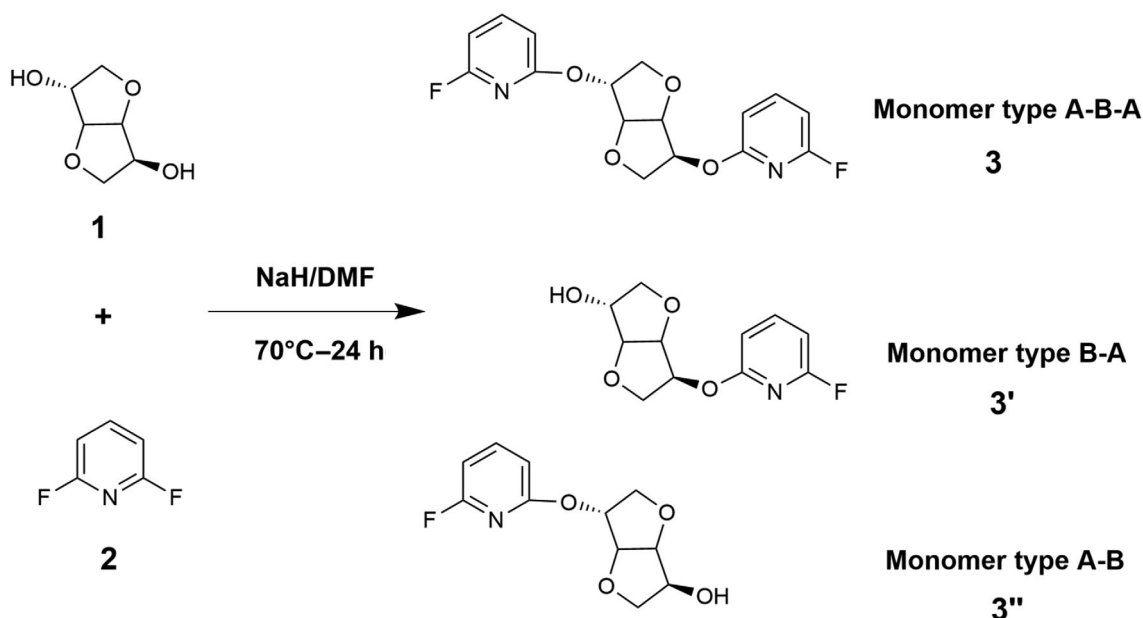


**FIGURE 3** Synthesis of the monomers (3, type A-B-A); (3', type B-A), and (3'', type A-B)

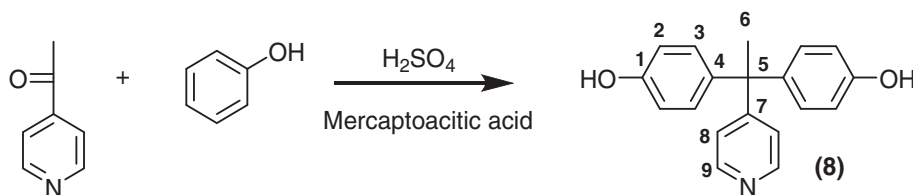


**FIGURE 4** Synthesis of bisphenol: 4,4'-(1-[pyridin-4-yl]ethane-1,1-diyl)diphenol (8)

mercaptoacetic acid (3.00 ml). The solution was stirred for a period of 15 min. Thereafter, sulfuric acid (100 ml) was added dropwise with a dropping funnel and then the reaction mixture was stirred overnight at room temperature. The reaction was monitored by <sup>1</sup>H NMR spectroscopy. After the reaction, the mixture was poured into 1 L of water. The obtained acidic solution was neutralized with a saturated solution of sodium carbonate. The obtained precipitated white powder was filtered, washed with water and then dried under vacuum at 80°C for 7 h. (yield = 55%).

<sup>1</sup>H NMR: (300 MHz, DMSO-d<sub>6</sub>); δ (ppm) = 9.25 (s, 2H<sub>1</sub>, OH); 8.45 (d, 2H<sub>9</sub>, <sup>3</sup>J<sub>9-8</sub> = 5.9 Hz); 7.02 (d, 2H<sub>8</sub>, <sup>3</sup>J<sub>8-9</sub> = 5.9 Hz); 6.82 (d, 4H<sub>3</sub>, <sup>3</sup>J<sub>3-2</sub> = 8.4 Hz); 6.70 (d, 4H<sub>2</sub>, <sup>3</sup>J<sub>2-3</sub> = 8.4 Hz); 1.94 (s, 3H<sub>6</sub>).

<sup>13</sup>C NMR: (75 MHz, DMSO-d<sub>6</sub>); δ (ppm) = 159.4 (C<sub>1</sub>); 156.4 (C<sub>7</sub>); 150.2 (C<sub>9</sub>); 138.8 (C<sub>3</sub>); 130.0 (C<sub>4</sub>); 124.4 (C<sub>8</sub>); 115.6 (C<sub>2</sub>); 51.5 (C<sub>5</sub>); 30.4 (C<sub>6</sub>).

### 2.2.3 | Synthesis of the polymers

(Figure 2) About 5 mmol of diol (1, 4, 5, 6, 7, and 8), 5 mmol of the difluoro monomer (3) and 11 mmol of potassium carbonate were added to 25% of DMF and heated to 140°C for 24 h, in a two-necked glass reactor equipped with a nitrogen inlet and a mechanical stirrer. The resulting viscous solution was poured slowly into methanol. Then

the resulting polymer was isolated by filtration, washed with cold methanol, and dried under vacuum at 80°C for 10 h. (yield 86%–96%).

### 2.3 | Characterization methods

The inherent viscosities (η) of the resulting polymers (P1–P6) were measured with Ubbelohde viscometer at 20°C in DMSO containing 2 vol% of trifluoroacetic acid (TFA).

TGA of the co-poly(ether pyridine)s were performed using a TA instruments apparatus (model 2950). Scans were run from 25 to 500°C at a heating rate of 10°C/min under a nitrogen atmosphere. The glass transition temperatures (T<sub>g</sub>) were obtained by DSC (Mettler Toledo DSC 822e). Scans were run from 25 to 300°C at a heating rate of 10°C/min in a nitrogen atmosphere.

The <sup>1</sup>H and <sup>13</sup>C NMR spectra were recorded at ambient temperature using a 300 MHz Bruker Advance 300 spectrometer, with DMSO-d<sub>6</sub> as solvent and tetramethylsilane as internal standard.

### 2.4 | Sorption studies

Sorption studies of benzene derivatives on the resulting polymers were carried out in a batch system by varying the contact time

(5–300 min) and the initial concentration of the targeted pollutants (5–50 mg L<sup>-1</sup>). The sorption experiments were conducted in glass flasks (20 ml) containing 60 mg of the sorbent, 10 ml of adsorbate benzene derivatives solution and 3 g of NaCl—the optimum amount for an optimum adsorption yield<sup>32,35</sup>—under constant agitation (stirring rate of 900 rpm) at room temperature (25 ± 1°C). The initial pH value of benzene derivatives solution was adjusted with orthophosphoric acid at pH = 2.

The samples of targeted pollutants after sorption tests were filtered with a PTFE 0.45 μm membrane filter and then analyzed using a HPLC/DAD equipment (wavelength: 210 nm), the analytical conditions were described in more detail in our previous work.<sup>32</sup>

The removal efficiency of benzene derivatives pollutants by the resulting poly(ether pyridine)s was calculated as follows:

$$\text{Sorption efficiency} = \left( \frac{C_i - C_t}{C_i} \right) * 100, \quad (1)$$

where  $C_i$  (mg L<sup>-1</sup>) is the initial concentration of the targeted pollutants and  $C_t$  (mg L<sup>-1</sup>) is their equilibrium concentration after adsorption.

The adsorbed amount of adsorbate per unit of mass of the sorbent,  $q_e$  (mg/g) was calculated as follows:

$$q_e = (C_0 - C_e) \times \frac{V}{m}, \quad (2)$$

where  $C_0$  and  $C_e$  are the initial and equilibrium concentrations of the targeted pollutants in mg L<sup>-1</sup>, respectively.  $V$  (L) is the volume of solution and  $m$  (g) is the amount of the dry polymer.

### 3 | RESULTS AND DISCUSSION

#### 3.1 | Synthesis and characterization of the polymers

A novel difluoro bio-based monomer (3, type A-B-A) was prepared via reaction of 2,6-difluoropyridine and isosorbide (Figure 3): in this

reaction applying non-stoichiometric ratio of 2,6-difluoropyridine versus isosorbide (2.5 to 1), it was the optimum ratio to reach the high-percent yield of the targeted monomer type A-B-A (3) compared to the monomer type B-A (3') and the monomer type A-B (3''). The novel difluoro A-B-A monomer was purified on a chromatography column to get 100% purity (<sup>1</sup>H NMR spectrum and <sup>13</sup>C NMR data of the monomer (3) is exemplified in Figure S1).

The main benefits of using this bio-based monomer containing pyridine units (containing nitrogen atoms, molecular symmetry, and aromaticity) and isosorbide (heterocyclic structure) is the improvement of the hydrophilicity, by producing polarized bond and improved hydrogen bond with oxygen and nitrogen atoms of the resulting polymers.

Another monomer was successfully synthesized, in one-step (Figure 4), for testing its effect on the resulting copolymer, a bisphenol containing a pyridine unit (8). The purity of this monomer was ascertained by NMR spectroscopy (Figure S2).

The novel bio-based difluoro monomer was incorporated in alternating copolymers structures by aromatic nucleophilic substitution (Figure 2).

As shown in Table 1, the resulting copolymers were obtained with satisfactory yields (86%–96%). The results demonstrate that moderate to high-molecular weights were obtained, with an inherent viscosity in the range of 0.75–1.23. The difference between these values can be explained by the reactivity of the used diols. The chemical composition of the prepared copolymers was ascertained by NMR spectroscopy. A detailed description of the <sup>1</sup>H NMR data recorded from the resulting polymers are given in Figure S2. The absence of end-groups on the NMR spectra can be explained by the high-molecular weight of the resulting polymers, as well as the possibility of the formation of cyclic molecular structures.<sup>39</sup> The <sup>1</sup>H NMR spectrum of the resulting polymer P6, for illustration, exhibits the characteristic protons of isosorbide (H1–H6), pyridine unit (H7–H9) and of the monomer (3) (H12–H16) (Figure S2).

In Table 1, the T<sub>g</sub> values of the resulting copolymers were found in the 121–143°C range (Figure S3). It can be noted that these values are suitable for engineering plastic to conserve their strength and shape at elevated temperature. The obtained T<sub>g</sub> values for P2 and P3 copolymers based on isomanide and isoidide respectively show clearly the effect of the chemical reactivity of these two isomers on thermal

**TABLE 1** Involved monomers in resulting polymers P1–P6, the obtained yields, their densities and their thermal properties

Polymer numbers	Monomers	Yield <sup>a</sup> (%)	$\eta_{inh}^b$ (dl/g)	T <sub>g</sub> <sup>c</sup> (°C)	Td <sub>5%</sub> <sup>d</sup> (°C)
P1	(1)/(3)	89	0.83	136	341
P2	(4)/(3)	86	0.75	132	340
P3	(5)/(3)	91	0.91	143	351
P4	(6)/(3)	93	1.12	121	347
P5	(7)/(3)	90	0.77	141	323
P6	(8)/(3)	96	1.23	142	352

<sup>a</sup>Precipitation into water and washing with methanol, evaporation under a vacuum at 80°C.

<sup>b</sup>Measured at 20°C with  $c = 2$  g L<sup>-1</sup> in DMSO containing 2 vol% of trifluoroacetic acid (TFA).

<sup>c</sup>Obtained by DSC with a heating rate of 10°C/min under nitrogen atmosphere.

<sup>d</sup>Td<sub>5%</sub> temperature of 5% weight loss, determined by TGA at 10°C min<sup>-1</sup> heating rate under inert gas.

behavior of the resulting copolymers. Such as, the most reactive isomer shows the highest  $T_g$  (143°C) compared to the lowest one (132°C). As observed in Table 1, a 5% weight loss, as a criterion for thermal stability, was in the 323–352°C range indicating that the prepared copolymers present good thermal behaviors (Figure S4).

### 3.2 | Comparative sorption efficiency of benzene derivatives pollutants on P1–P6 polymers

Adsorption is based only on physical or noncovalent interaction between the polymer and the pollutant molecules; it takes place at the opened surface of the sorbent particles. These interactions can be due to many interactions such as  $\pi$ - $\pi$  interactions, hydrophobic interactions, weak Van der Waals interactions, H-bonding and even electrostatic interactions.

The adsorption efficiency of P1–P6 polymers was observed after three time periods (0.33, 1, and 24 h), as described in the experimental section, for an initial aromatic pollutant concentration of 5 mg L<sup>-1</sup> (Table 2).

The chemical structures of the targeted pollutants were investigated as illustrated in Figure 2, where the pollutants were classified according to their value of the octanol–water partitioning (log Kow). As well as, we present their water solubility values in Table 2 (Experimental values are used when available, otherwise ChemAxon estimated values are presented).

Among all the pollutants used, (E)anethol which presents the highest Log Kow and the lowest solubility in water (Log Kow = 3.3; Solubility in water at 20°C = 0.11 g L<sup>-1</sup>) was completely adsorbed (at a sorption efficiency of 100%) by all the polymeric phases within only 20 min with no regard to their molecular structures. This clearly shows that all the sorbents used were able to establish stronger interactions with the molecules of anethol than those that already established by this molecule with the water molecules (generally weak interactions like Van der Waals due to the anethol nonpolar nature). On the other side, the sorption results have shown that the 4-hydrobenzoic acid was the most persistent polluting compound in water. In fact, most of the polymeric phases were unable to efficiently remove this pollutant from water. The high persistence of the 4-hydrobenzoic acid can be due to the fact that it is the most polar compound (Log Kow = 1.15; Solubility in water at 25°C = 50 g L<sup>-1</sup>) among all the sorbates, meaning that it can establish strong or relatively high-energy interactions with the water molecules (H-bonding). In order to fully remove this pollutant from water, the sorbent has to establish stronger interactions with the 4-hydrobenzoic acid. The sorption results have shown that most of the sorbents used were not able to establish strong interactions with the 4-hydrobenzoic acid and thus its adsorption efficiency was low with most polymers, with the exception of P6. In fact, this polymer was the only sorbent able to establish strong enough interaction with this pollutant.

This approach allowed us to understand the importance of the chemical structures of the sorbates. In fact, the sorption process depends strongly on the hydrophilicity and on the solubility of the

pollutant in water, the more the sorbate is hydrophilic and soluble in water the more it establishes strong interactions with the molecules of water and thus the more difficult it can be sorbed onto the solid phase.

It was found that after 1 h of contact with polymer P1, only 12% of the P-hydroxybenzoic acid (log Kow = 1.58) was adsorbed whereas 100% of the (E) anethol (log Kow = 3.3) was retained. It can be seen also that the sorption efficiency of the polymers based on dianhydrohexitols isomers (Family A: isosorbide: P1/isomanide: P2/isoidide P3), have the same sorption efficiency for the targeted pollutants. The stereochemistry of the dianhydrohexitols has no influence on the sorption efficiency of the resulting polymers.

For the Family B, polymers based bisphenols, have sorption results increased following the order P4 (based bisphenol A) < P5 (based bisphenol S) < P6 (based bisphenol containing pyridine units). These results can be explained by the effect of the functional group between the two benzene rings. For P4, the two methyl in the bisphenol A structure make the polymer more hydrophobic and thus the contact surface with the targeted pollutants is considerably decreased. In the case of P5, sulfone group in the bisphenol S structure make the polymer more hydrophilic, which explains that the sorption efficiency is close to that obtained with the polar structure based on dianhydrohexitols. The most efficient polymer, polymer P6, 93% of the p-hydroxybenzoic acid was adsorbed after 1 h and 100% of the (E) anethol. This polymer contains 4,4'-(1-[pyridin-4-yl]ethane-1,1-diyl)diphenol units and monomer 3, which gives good sorption efficiency due to the different types of interactions:  $\pi$ - $\pi$  interactions and H-bonding. According to the structure of the Family A polymers (containing atoms of oxygen, nitrogen, not aromatic rings), their structure is properly more hydrophilic than that of the most efficient adsorbent P6. According to these results, there is another parameter, other than the hydrophilicity, that can affect the sorption efficiency of the linear polymers. In fact, the distance or the interaction between polymer chains can be adjusted to be smaller or larger by modifying the structure of polymer, precisely in our case the modification of the repeating units of polymers. Such as, more compact the polymer chains, lower the sorption efficiency, less compact the polymer chain, higher the sorption efficiency. In our work, the bisphenol-based polymer (Family B), including a 3D spacer (Figure 5) present a similar or a higher sorption efficiency than the bio-based polymers (Family A), because their structure is less compact and more porous structure.

Based on the results mentioned above, the polymer P6 was selected as being the most efficient polymer, able to adsorb the maximum of pollutant molecules after 1 h of contact.

### 3.3 | Sorption characteristics of P6 polymer

#### 3.3.1 | Effect of initial concentration of the pollutant

The initial concentration of pollutant is an important factor affecting the mass transfer of the molecules between the aqueous and the solid

**TABLE 2** Sorption efficiency (%) of benzene derivatives pollutants on P1–P6 polymers after different time durations. Experimental conditions: targeted pollutant concentration: 5 mg L<sup>-1</sup>; NaCl concentration: 300 g L<sup>-1</sup>; 60 mg of sorbent, pH 2

Polymers	P1		P2		P3		P4		P5		P6									
	0.33	1	24	20	21	23	34	21	25	50	18	19	23	20	23	54	93 ± 4.65	95 ± 4.75	95 ± 4.75	
Time (h)	0.33	1	24	0.33	1	24	0.33	1	24	0.33	1	24	0.33	1	24	0.33	1	24		
<b>Targeted pollutants</b>																				
<b>Water solubility</b>																				
P-hydroxybenzoic acid	50 g L <sup>-1</sup>		50 g L <sup>-1</sup>		50 g L <sup>-1</sup>		50 g L <sup>-1</sup>		50 g L <sup>-1</sup>		50 g L <sup>-1</sup>		50 g L <sup>-1</sup>		50 g L <sup>-1</sup>		50 g L <sup>-1</sup>		50 g L <sup>-1</sup>	
	(25°C)		(25°C)		(25°C)		(25°C)		(25°C)		(25°C)		(25°C)		(25°C)		(25°C)		(25°C)	
Cafeic acid	<1 g L <sup>-1</sup>		<1 g L <sup>-1</sup>		<1 g L <sup>-1</sup>		<1 g L <sup>-1</sup>		<1 g L <sup>-1</sup>		<1 g L <sup>-1</sup>		<1 g L <sup>-1</sup>		<1 g L <sup>-1</sup>		<1 g L <sup>-1</sup>		<1 g L <sup>-1</sup>	
	(22°C)		(22°C)		(22°C)		(22°C)		(22°C)		(22°C)		(22°C)		(22°C)		(22°C)		(22°C)	
Ferrulic acid	5.97 g L <sup>-1</sup>		5.97 g L <sup>-1</sup>		5.97 g L <sup>-1</sup>		5.97 g L <sup>-1</sup>		5.97 g L <sup>-1</sup>		5.97 g L <sup>-1</sup>		5.97 g L <sup>-1</sup>		5.97 g L <sup>-1</sup>		5.97 g L <sup>-1</sup>		5.97 g L <sup>-1</sup>	
	(25°C)		(25°C)		(25°C)		(25°C)		(25°C)		(25°C)		(25°C)		(25°C)		(25°C)		(25°C)	
Benzoic acid	3.4 g L <sup>-1</sup>		3.4 g L <sup>-1</sup>		3.4 g L <sup>-1</sup>		3.4 g L <sup>-1</sup>		3.4 g L <sup>-1</sup>		3.4 g L <sup>-1</sup>		3.4 g L <sup>-1</sup>		3.4 g L <sup>-1</sup>		3.4 g L <sup>-1</sup>		3.4 g L <sup>-1</sup>	
	(25°C)		(25°C)		(25°C)		(25°C)		(25°C)		(25°C)		(25°C)		(25°C)		(25°C)		(25°C)	
Anisic acid	0.53 g L <sup>-1</sup>		0.53 g L <sup>-1</sup>		0.53 g L <sup>-1</sup>		0.53 g L <sup>-1</sup>		0.53 g L <sup>-1</sup>		0.53 g L <sup>-1</sup>		0.53 g L <sup>-1</sup>		0.53 g L <sup>-1</sup>		0.53 g L <sup>-1</sup>		0.53 g L <sup>-1</sup>	
	(37°C)		(37°C)		(37°C)		(37°C)		(37°C)		(37°C)		(37°C)		(37°C)		(37°C)		(37°C)	
Toluic acid	0.34 g L <sup>-1</sup>		0.34 g L <sup>-1</sup>		0.34 g L <sup>-1</sup>		0.34 g L <sup>-1</sup>		0.34 g L <sup>-1</sup>		0.34 g L <sup>-1</sup>		0.34 g L <sup>-1</sup>		0.34 g L <sup>-1</sup>		0.34 g L <sup>-1</sup>		0.34 g L <sup>-1</sup>	
	(25°C)		(25°C)		(25°C)		(25°C)		(25°C)		(25°C)		(25°C)		(25°C)		(25°C)		(25°C)	
P-chlorobenzoic acid	72 mg L <sup>-1</sup>		72 mg L <sup>-1</sup>		72 mg L <sup>-1</sup>		72 mg L <sup>-1</sup>		72 mg L <sup>-1</sup>		72 mg L <sup>-1</sup>		72 mg L <sup>-1</sup>		72 mg L <sup>-1</sup>		72 mg L <sup>-1</sup>		72 mg L <sup>-1</sup>	
	(25°C)		(25°C)		(25°C)		(25°C)		(25°C)		(25°C)		(25°C)		(25°C)		(25°C)		(25°C)	
Eugenol	2.46 g L <sup>-1</sup>		2.46 g L <sup>-1</sup>		2.46 g L <sup>-1</sup>		2.46 g L <sup>-1</sup>		2.46 g L <sup>-1</sup>		2.46 g L <sup>-1</sup>		2.46 g L <sup>-1</sup>		2.46 g L <sup>-1</sup>		2.46 g L <sup>-1</sup>		2.46 g L <sup>-1</sup>	
	(25°C)		(25°C)		(25°C)		(25°C)		(25°C)		(25°C)		(25°C)		(25°C)		(25°C)		(25°C)	
(E) anethol	0.11 g L <sup>-1</sup>		0.11 g L <sup>-1</sup>		0.11 g L <sup>-1</sup>		0.11 g L <sup>-1</sup>		0.11 g L <sup>-1</sup>		0.11 g L <sup>-1</sup>		0.11 g L <sup>-1</sup>		0.11 g L <sup>-1</sup>		0.11 g L <sup>-1</sup>		0.11 g L <sup>-1</sup>	
	(20°C)		(20°C)		(20°C)		(20°C)		(20°C)		(20°C)		(20°C)		(20°C)		(20°C)		(20°C)	

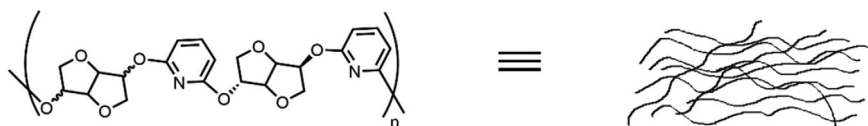
Note: Bold values are sorption efficiency obtained with P6 polymer, this one was further selected for the study of sorption characteristics.

phases. The effect of initial concentration on the sorption efficiency of the more efficient sorbent, polymer P6 was studied toward two pollutants (p-hydroxybenzoic acid and toluic acid). These pollutants are subject of many interests and are the metabolites of many organic hazard pollutants. The sorption experiments of the target pollutants were carried out by varying pollutant concentrations in the range of 5–50 mg L<sup>-1</sup> on 60 mg of the polymer P6 as a function of time (Figure 6).

As shown in Figure 6, a rapid initial sorption efficiency of the two-targeted pollutants took place for all the tested initial

concentration followed by a slower removal rate. These results can be explained by the presence free active sites allowing strong interaction with the targeted molecules. For 5 and 10 mg L<sup>-1</sup> concentrations, the sorption efficiency approaches the equilibrium after 60 min. For the other tested concentrations, the sorption needs more time to reach equilibrium. These results imply that the ratio of active site to the total molecules in the solution at low-initial concentration is high. It can be seen also that the more hydrophilic pollutant (p-hydroxybenzoic acid) presents the slower sorption rate compared to that of the more hydrophobic one (toluic acid).

### Family A



### Family B

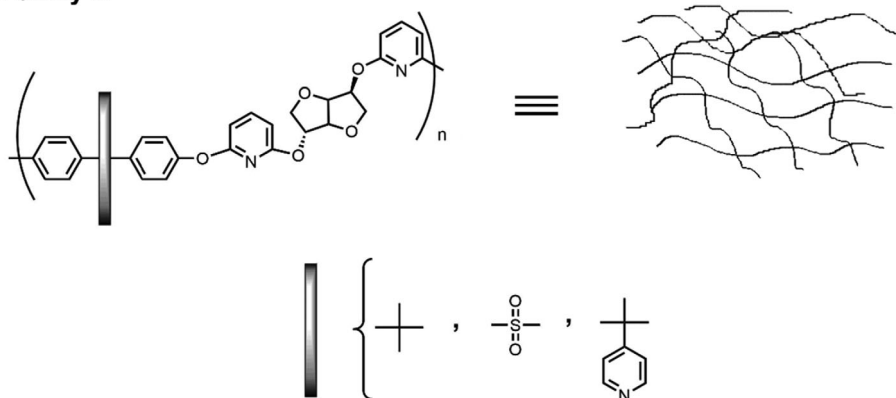


**FIGURE 5** Compared compactness of the polymer chains: bio-based polymers (Family A), bisphenol-based polymer (Family B)

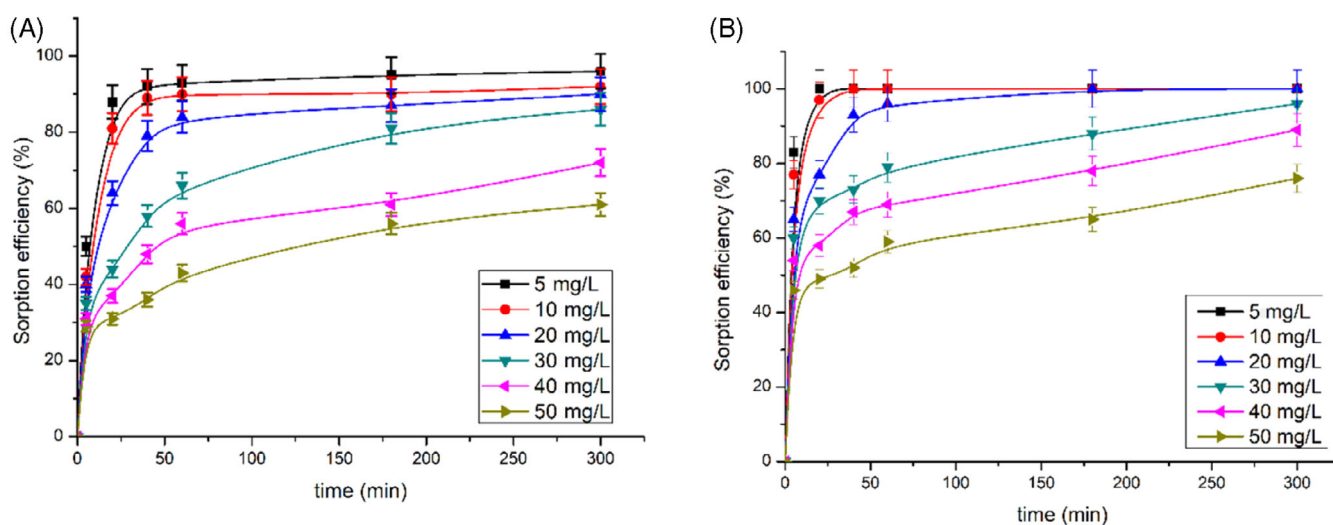


**FIGURE 6** Effect of initial concentration of the pollutant on the sorption efficiency of (A) p-hydroxybenzoic acid and (B) toluic acid. Experimental conditions: 60 mg of polymer P6; NaCl concentration: 300 g L<sup>-1</sup>; pH 2; stirring speed = 900 rpm; at room temperature



### 3.3.2 | Sorption kinetic modeling

In order to investigate the sorption kinetics of p-hydroxybenzoic acid and toluic acid on the poly(ether pyridine) P6, three widely used kinetic models were applied to describe the sorption process, pseudo-first-order model,<sup>40</sup> pseudo-second order model,<sup>41</sup> and intraparticle diffusion model.<sup>42</sup> The nonlinear form expressions of the pseudo first-order and pseudo-second-order, and the linear form of the intraparticle diffusion models are represented by Equations (3), (4), and (5), respectively.

$$Qt = Qe(1 - e^{-k_1 t}), \quad (3)$$

$$Qt = \frac{k_2 t Qe^2}{1 + k_2 Qe t}, \quad (4)$$

$$Qt = Kp * (t^{1/2}) + C, \quad (5)$$

where  $Qt$  and  $Qe$  are the quantity of pollutant adsorbed by the polymer P6 (in mg/g) respectively at time  $t$  and at equilibrium.  $k_1$  and  $k_2$  are respectively the pseudo-first-order rate constant ( $\text{min}^{-1}$ ) and the pseudo-second-order rate constant ( $\text{mg mg}^{-1} \text{min}^{-1}$ ).  $Kp$  is the intraparticle diffusion rate parameter.  $C$  is the thickness of pollutants species at the adsorbent surface.

In order to quantitatively compare the applications of the kinetic model, the regression.

coefficients ( $R^2$ ) were calculated by the following formula:

$$R^2 = \frac{\sum |Qt_{\text{exp}} - Qt_{\text{aver,exp}}|^2}{\sum |Qt_{\text{exp}} - Qt_{\text{aver,exp}}|^2 + \sum |Qt_{\text{exp}} - Qt_{\text{mod}}|^2}, \quad (6)$$

where  $Qt_{\text{exp}}$  and  $Qt_{\text{mod}}$  (mg/g) are the sorption quantities, at time  $t$ , experimental and predicted by the models, respectively;  $Qt_{\text{aver,exp}}$  is the average of  $Qt_{\text{exp}}$ .

The nonlinear (a) pseudo-first-order and (b) pseudo-second-order (c) intra-particle diffusion models for the sorption kinetics of the four selected target pollutants onto P6, for different initial concentrations, are presented in Figures S5 and S6.

The sorption kinetics data are fitted with pseudo-first-order and pseudo-second-order models. The obtained kinetic parameters and correlation coefficients ( $R^2$ ) by nonlinear regressions are presented in Table S1. The correlation coefficients ( $R^2$ ) of the pseudo-second-order model for both target pollutants are higher than that of the pseudo-first order model. Moreover, the experimental sorption capacities ( $Qe_{\text{exp}}$ ) for both target pollutants are very close to the calculated values ( $Qe_{\text{cal}}$ ) from the pseudo-second-order model, indicating that the pseudo-second-order model is well suitable for describing the sorption process.

The intraparticle diffusion model was applied to determine the effect of intraparticle diffusion on sorption process that is generally controlled by liquid mass transport or intraparticle mass transport and also gives an idea about the mechanism steps that

took place in this process. The linear plots of intraparticle diffusion model are shown in Figures S5c and S6c. From this model it comes that adsorption process was carried out in three consecutive steps:

1. Instantaneous adsorption of adsorbate on the adsorbent surface.
2. Diffusion of adsorbate molecules in adsorbent pores.
3. Adsorption of adsorbate molecules on the inner surface of the adsorbent pores.

The values of intraparticle rate  $k_{\text{int}}$  (Table S1) decrease with the passage of the first step ( $k_{\text{int1}}$ ) toward the second step ( $k_{\text{int2}}$ ) and toward the third step ( $k_{\text{int3}}$ ). From this results, it comes that the sorption mechanism is mainly governed by boundary layer diffusion and intraparticle diffusion. Similar sorption mechanism was observed in the work of<sup>35</sup> for adsorption of p-hydroxybenzoic acid, toluic acid, deisopropylatrazine, 2,4,6-trichlorophenol on a bio-sourced poly(ether-pyridine).

### 3.3.3 | Sorption isotherms

Sorption isotherm models are widely used to describe the sorption process and investigate the sorption mechanisms. Two sorption isotherms models, the Freundlich and Langmuir models were used for fitting the experimental data. The nonlinear Freundlich isotherm model is represented by Equation (7):

$$Qe = K_F C_e^{1/n_F}, \quad (7)$$

where  $Qe$  is the sorbed amount of the pollutant at equilibrium (in mg/g),  $C_e$  is the concentration of pollutant solution at equilibrium (in  $\text{mg L}^{-1}$ ),  $K_F$  ( $\text{mg/g} [\text{mg L}^{-1}]^{-1/n_F}$ ) is the Freundlich constant related to sorption capacity and  $n_F$  the heterogeneous factor related to the sorption intensity.

The Langmuir isotherm model is based on the following assumptions: (1) the sorption takes place as a monolayer on the sorbent, and only one molecule is adsorbed at each adsorption site (2) there is no interaction between the sorbed molecules, (3) the enthalpy values of all sorbed molecules are equal. The nonlinear Langmuir isotherm model is given by Equation (8):

$$Qe = (C_e K_L Q_{\text{max}}) / (1 + K_L C_e), \quad (8)$$

where  $Q_{\text{max}}$  is the maximum amount of sorption with a complete monolayer coverage on the sorbent surface (in mg/g), and  $K_L$  is the Langmuir sorption constant (L/mg).

In order to quantitatively compare the applications of the isotherm model, the regression.

coefficients ( $R^2$ ) were calculated by the following formula:

$$R^2 = \frac{\sum |Qe - Qe_{\text{aver}}|^2}{\sum |Qe - Qe_{\text{aver}}|^2 + \sum |Qe - Qe_{\text{mod}}|^2}, \quad (9)$$

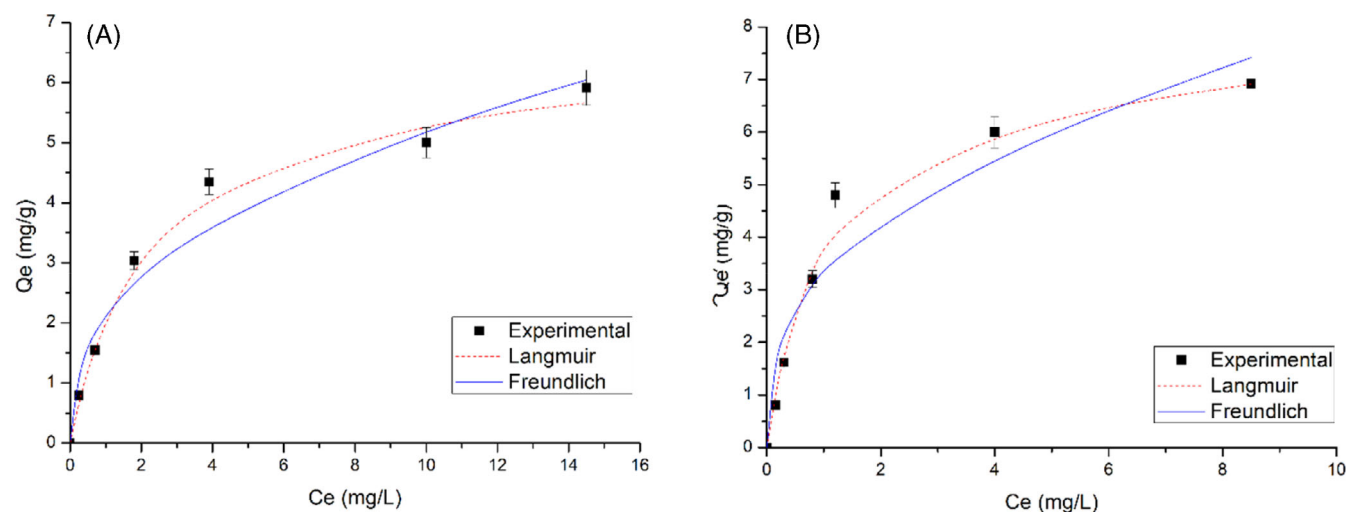


**FIGURE 7** Nonlinear fitting curves of the Freundlich and Langmuir sorption isotherms at 25°C: (A) *p*-hydroxybenzoic acid, (B) toluic acid; Experimental conditions: initial concentration = 5–50 mg L<sup>-1</sup>; NaCl concentration: 300 g L<sup>-1</sup>; pH 2; stirring speed = 900 rpm

**TABLE 3** Langmuir and Freundlich isotherm constants for sorption of *p*-hydroxybenzoic acid and toluic acid onto P6 and regression coefficients of the fitting of the experimental data

Pollutants	Log Kow	Langmuir constants			Freundlich constants		
		Q <sub>max</sub> (mg/g)	K <sub>L</sub> (L/mg)	R <sup>2</sup>	K <sub>F</sub> (L/g)	1/n	R <sup>2</sup>
<i>p</i> -hydroxybenzoic acid	1.58	6.462	0.486	0.993	2.178	0.382	0.965
Toluic acid	2.35	7.717	1.007	0.988	3.399	0.365	0.928

**TABLE 4** Comparison of 1/*n* values, inverse of the sorption intensity, for different sorbents for benzoic acid

Adsorbent	Benzoic acid
Biochar	1/ <i>n</i> = 0.62 <sup>21</sup>
Cross-linked methacrylate resin	1/ <i>n</i> = 0.64 <sup>43</sup> Q <sub>max</sub> = 245 mg/g <sup>43</sup>
Bio-based poly(ether-pyridine)	1/ <i>n</i> = 0.311 <sup>35</sup> Q <sub>max</sub> = 4.941 mg/g <sup>35</sup>
Polymer P6 (this work)	1/ <i>n</i> = 0.382 Q <sub>max</sub> = 6.462 mg/g

where  $Q_e$  is the experimental sorbed amount at equilibrium (mg/g),  $Q_e$  mod is the sorbed amount predicted by the Langmuir or Freundlich model (mg/g) and  $Q_{eaver}$  is the average of the experimental sorbed amount.

As shown in Figure 7, the fit with Langmuir model appears better than that with Freundlich model for (a) *p*-hydroxybenzoic acid and (b) toluic acid. This point is verified by the found values of  $R^2$  in Table 3. The lower value of 1/*n* and the higher value of  $Q_{max}$  for toluic acid, compared to those of *p*-hydroxybenzoic, show that its sorption on P6 is easier.

The characteristics of the adsorption of benzoic acid on different adsorbents are compared in Table 4. When comparing the 1/*n* values

for benzoic acid for biochar (0.62), cross-linked methacrylate resin (0.64) and for bio-based poly(ether-pyridine) (0.311), to the 1/*n* value for polymer P6 (0.365), it appears that the alternating co-poly(ether pyridine) P6 presents a high affinity for this compound. Nevertheless, P6 polymer presents a very low sorption capacity, 6.46 mg/g, compared to the cross-linked methacrylate resin and a higher sorption capacity than bio-based poly(ether-pyridine). This higher sorption capacity compared to the bio-based poly(ether-pyridine) can be explained by the difference in the structures. In fact, 3D spacers in the P6 copolymer make this polymeric phase more available for  $\pi$ - $\pi$  interactions, due its lower compactness.

## 4 | CONCLUSION

The developed adsorbents are new alternating copolymers derived from isosorbide and 2,6-difluoropyridine. Six different monomers, dianhydrohexitols isomers and bisphenol derivatives, were synthesized in order to make it possible to study their hydrophilic and hydrophobic effect on the sorption efficiency of the resulting polymeric phases. The structure of these copolymers were characterized by <sup>1</sup>H NMR spectroscopy, DSC and ATG. These polymers have a good thermal stability, a 5% weight loss is observed above 340°C. Benzene derivative sorption efficiency of polymers was successfully measured using high-performance liquid chromatography. The results show the

high sorption efficiency of the resulting polymer (P6) toward all the aromatic compounds (more than 95% after 1 h) with log  $K_{ow}$  between 1.43 and 3.3. The sorption kinetic data, using polymer P6 as sorbent, fitted well to a pseudo-second-order model. Sorption equilibrium data reveal that the sorption mechanism obeys better to Langmuir isotherm model that assume the adsorption was made onto a homogenous surface, sorption sites presenting a high affinity compared to that of current adsorbents such as biochar and methacrylate resin. The preparation of microporous materials based on the polymer P6 will be able to increase its sorption efficiency and make them promising polymers to have applications in water remediation or in SPME analytical devices.

#### DATA AVAILABILITY STATEMENT

The data that support the findings of this study are available from the corresponding author upon reasonable request.

#### ORCID

Taha Chabbah  <https://orcid.org/0000-0001-7361-7026>

Saber Chatti  <https://orcid.org/0000-0001-8815-8109>

Nicole Jaffrezic-Renault  <https://orcid.org/0000-0003-1354-9273>

#### REFERENCES

- Wang H, Wang D, Tian T, Ren W. Removal of organic compounds containing a benzene ring from water by adsorptive micellar flocculation. *J Surfact Deterg.* 2019;22:161-174. doi:10.1002/jsde.12209
- Abdel-Shafy HI, Mansour MSM. A review on polycyclic aromatic hydrocarbons: source, environmental impact, effect on human health and remediation. *Egypt J Petrol.* 2016;25:107-123. doi:10.1016/j.ejpe.2015.03.011
- Mao G, Hu H, Liu X, Crittenden J, Huang N. A bibliometric analysis of industrial wastewater treatments from 1998 to 2019. *Environ Pollut.* 2020;7:115785. doi:10.1016/j.envpol.2020.115785
- Anku WW, Mamo MA, Govender PP. Phenolic compounds in water: sources, reactivity, toxicity and treatment methods. In: Soto-Hernandez M, Palma-Tenango M, Garcia-Mateos MR, eds. *Book: Phenolic Compounds - Natural Sources, Importance and Applications.* IntechOpen; 2017:420-443. doi:10.5772/66927
- Hendryx M, Conle J, Fedorko E, Luo J, Armistead M. Permitted water pollution discharges and population cancer and non-cancer mortality: toxicity weights and upstream discharge effects in US rural-urban areas. *Int J Health Geogr.* 2012;11:11-15. doi:10.1186/1476-072X-11-9
- Afsar B, Rengin EA, Kanbay A, Covic A, Ortiz A, Kanbay M. Air pollution and kidney disease: review of current evidence. *Clin Kidney J.* 2019;12:19-32. doi:10.1093/ckj/sfy111
- Epstein AC. The human health implications of oil and natural gas development. In: Schug K, Hildenbrand Z, eds. *Environmental Issues Concerning Hydraulic Fracturing in Advances in Chemical Pollution. Environmental Management and Protection.* Vol 1. Elsevier; 2017:113-145. doi:10.1016/bs.apmp.2017.08.002
- Alvaro M, García H, Sanjuán A, Esplá M. Hydroxyalkylation of benzene derivatives by benzaldehyde in the presence of acid zeolites. *Appl Catal A.* 1998;175:105-112. doi:10.1016/S0926-860X(98)00213-0
- Bradley PM, Journey CA, Romanok KM, et al. Expanded target-chemical analysis reveals extensive mixed-organic-contaminant exposure in U.S. streams. *Environ Sci Technol.* 2017;51:4792-4802. doi:10.1021/acs.est.7b00012
- Devier MH, Mazellier P, Ait-Aissa S, Budzinski H. New challenges in environmental analytical chemistry: identification of toxic compounds in complex mixtures. *C R Chim.* 2011;14:766-779. doi:10.1016/j.crci.2011.04.006
- Zazouli MA, Kalankesh LR. Removal of precursors and disinfection byproducts (DBPs) by membrane filtration from water. *J Environ Health Sci Eng.* 2017;15:1-15. doi:10.1186/s40201-017-0285-z
- Wang N, Zhao Q, Zhang A. Catalytic oxidation of organic pollutants in wastewater via a Fenton-like process under the catalysis of HNO<sub>3</sub>-modified coal fly ash. *RSC Adv.* 2017;7:27619-27628. doi:10.1039/C7RA04451H
- El-taliawy H, Ekblad M, Nilsson F, et al. Ozonation efficiency in removing organic micro pollutants from wastewater with respect to hydraulic loading rates and different wastewaters. *Chem Eng J.* 2017; 325:310-321. doi:10.1016/j.cej.2017.05.019
- Yuan X, Floresyona D, Aubert PH, et al. Photocatalytic degradation of organic pollutant with polypyrrole nanostructures under UV and visible light. *Appl Catal B Environ.* 2019;242:284-292. doi:10.1016/j.apcatb.2018.10.002
- Cai J, Zhou M, Pan Y, Du X, Lu X. Extremely efficient electrochemical degradation of organic pollutants with co-generation of hydroxyl and sulfate radicals on blue-TiO<sub>2</sub> nanotubes anode. *Appl Catal B-Environ.* 2019;257:117902-117915. doi:10.1016/j.apcatb.2019.117902
- Kang JW. Removing environmental organic pollutants with bioremediation and phytoremediation. *Biotechnol Lett.* 2014;36:1129-1139. doi:10.1007/s10529-014-1466-9
- Sandau CD, Sjödin A, Davis MD, et al. Comprehensive solid-phase extraction method for persistent organic pollutants. Validation and application to the analysis of persistent chlorinated pesticides. *Anal Chem.* 2003;75:71-77. doi:10.1021/ac026121u
- Mejía-Morales C, Hernández-Aldana F, Cortés-Hernández DM. Assessment of biological and persistent organic compounds in hospital wastewater after advanced oxidation process UV/H<sub>2</sub>O<sub>2</sub>/O<sub>3</sub>. *Water Air Soil Pollut.* 2020;231:89-99. doi:10.1007/s11270-020-4463-8
- Xiang Q, Nomura Y, Fukahori S, Mizuno T, Tanaka H, Fujiwara T. Innovative treatment of organic contaminants in reverse osmosis concentrate from water reuse. *Curr Pollut Rep.* 2019;5:294-307. doi:10.1007/s40726-019-00119-2
- Patiño Y, Díaz E, Ordóñez S, Gallegos-Suarez E, Guerrero-Ruiz A, Rodríguez-Ramos I. Adsorption of emerging pollutants on functionalized multiwall carbon nanotubes. *Chemosphere.* 2015;136: 174-180. doi:10.1016/j.chemosphere.2015.04.089
- Shimabuku KK, Paige JM, Luna-Aguero M, Summers RS. Simplified modeling of organic contaminant adsorption by activated carbon and biochar in the presence of dissolved organic matter and other competing adsorbates. *Environ Sci Technol.* 2017;51:10031-10040. doi:10.1021/acs.est.7b00758
- Goworek J, Ościk J, Kusak R. Adsorption of benzene derivatives from binary and ternary solutions in benzene and n-heptane on silica gel. *J Coll Interf Sci.* 1985;103(2):392-399. doi:10.1016/0021-9797(85)90117-1
- Awad AM, Shaikh SMR, Jalab R, et al. Adsorption of organic pollutants by natural and modified clays: a comprehensive review. Separation and purification technology. *Sep Purif Technol.* 2019;228:115719. doi:10.1016/j.seppur.2019.115719
- Jiang N, Shang R, Heijman SGJ, Rietveld LC. High-silica zeolites for adsorption of organic micro-pollutants in water treatment. *Water Res.* 2014;144:145-161. doi:10.1016/j.watres.2018.07.017
- Xie LH, Liu XM, He T, Li JR. Metal-organic frameworks for the capture of trace aromatic volatile organic compounds. *Chem.* 2018;4: 1911-1927. doi:10.1016/j.chempr.2018.05.017
- Nguyen NT, Dao TH, Truong TT, Nguyen TMT, Pham D. Adsorption characteristic of ciprofloxacin antibiotic onto synthesized alpha alumina nanoparticles with surface modification by

- polyanion. *J Mol Liq.* 2020;309:113150-113107. doi:10.1016/j.molliq.2020.113150
27. Huang Q, Chai K, Zhou L, Ji H. A phenyl-rich  $\beta$ -cyclodextrin porous crosslinked polymer for efficient removal of aromatic pollutants: insight into adsorption performance and mechanism. *Chem Eng J.* 2020;387:124020-124031. doi:10.1016/j.cej.2020.124020
28. Zeng X, Wang Y, Shu Z, Huang J. Hydroquinone-modified hyper-crosslinked polymer and its adsorption of aniline. *Chem Eng J Adv.* 2020;1:100004-100012. doi:10.1016/j.cej.2020.100004
29. Sheng X, Shi H, Yang L, Shao P, Yu K, Luo X. Rationally designed conjugated microporous polymers for contaminants adsorption. *Sci Tot Environ.* 2021;750:141683. doi:10.1016/j.scitotenv.2020.141683
30. Frimmel FH, Assenmacher M, Sørensen M, Abbt-Braun G, Gräbe G. Removal of hydrophilic pollutants from water with organic adsorption polymers. *Chem Eng Process.* 1999;38:601-610. doi:10.1016/S0255-2701(99)00061-6
31. Majumdar S, Moral R, Mahanta D. Rapid mixing polymerization: a simple method for preparation of free standing polypyrrole film and powder for the removal of anionic pollutants. *Colloids Surf A Physicochem Eng Asp.* 2020;595:124643-124655. doi:10.1016/j.colsurfa.2020.124643
32. Chabbah T, Abderrazak H, Saint Martin P, Casabianca H, Kricheldorf HR, Chatti S. Synthesis of glux based polymers for removal of benzene derivatives and pesticides from water. *Polym Adv Technol.* 2020;31:2339-2350. doi:10.1002/pat.4953
33. Zeng C, Seino H, Ren J, Hatanaka K, Yoshie N. Self-healing bio-based furan polymers crosslinked with various bis-maleimides. *Polymer.* 2013;54:5351-5357. doi:10.1016/j.polymer.2013.07.059
34. Fenouillot F, Rousseau A, Colomines G, Saint-Loup R, Pascault JP. Polymers from renewable 1,4:3,6-dianhydrohexitols (isosorbide, isomannide and isoidide). *Prog Polym Sci.* 2010;35:578-622. doi:10.1016/j.progpolymsci.2009.10.001
35. Gomri M, Abderrazak H, Chabbah T, et al. Adsorption characteristics of aromatic pollutants and their halogenated derivatives on bio-based poly(ether-pyridine)s. *J Environ Chem Eng.* 2020;8:104333-104347. doi:10.1016/j.jece.2020.104333
36. Jlalía I, Zouaoui F, Chabbah T, et al. Adsorption characteristics of WFD heavy metal ions on new biosourced polyimide films determined by electrochemical impedance spectroscopy. *J Inorg Org Polym Mater.* 2021;31:2471-2482. doi:10.1007/s10904-020-01842-w
37. Khodami S, Babanzadeh S, Mehdipour-Ataei S. Improving the performance of novel polysulfone-based membrane via sulfonation method: application to water desalination. *J Appl Polym Sci.* 2019;137:48568-48578. doi:10.1002/app.48568
38. Chatti S, Casabianca H, Mercier R. Use of a polymer containing units derived from 1,4:3,6-dianhydrohexitol for adsorbing chemical compounds, Patent number WO2019/110759 A1, 2019.
39. Kricheldorf HR, Chatti S, Schwarz G, Kruger RP. Macrocycles 27: cyclic aliphatic polyesters of isosorbide. *J Polym Sci A Polym Chem.* 2003;41:3414-3424. doi:10.1002/pola.10933
40. Liu C, Omer AM, Kun OX. Adsorptive removal of cationic methylene blue dye using carboxymethyl cellulose/k-carrageenan/activated montmorillonite composite beads: isotherm and kinetic studies. *Int J Bio Macromol.* 2018;106:823-833. doi:10.1016/j.ijbiomac.2017.08.084
41. Tien C, Ramarao BV. On the significance and utility of the Lagergren model and the pseudosecond-order model of batch adsorption. *Sep Sci Technol.* 2017;52:975-986. doi:10.1080/01496395.2016.1274327
42. Laabd M, El Jaouhari A, Ait Haki M, et al. Simultaneous removal of benzene polycarboxylic acids from water by polypyrrole composite filled with a cellulosic agricultural waste. *J Environ Chem Eng.* 2016;4:1869-1879. doi:10.1016/j.jece.2016.03.015
43. Shao L, Li Y, Zhang T, Liu M, Huang J. Controllable synthesis of polar modified hyper-cross-linked resins and their adsorption of 2-naphthol and 4-hydroxybenzoic acid from aqueous solution. *Ind Eng Chem Res.* 2017;56:2984-2992. doi:10.1021/acs.iecr.6b04953

#### SUPPORTING INFORMATION

Additional supporting information may be found in the online version of the article at the publisher's website.

**How to cite this article:** Jlalía I, Chabbah T, Chatti S, et al. Alternating bio-based pyridinic copolymers modified with hydrophilic and hydrophobic spacers as sorbents of aromatic pollutants. *Polym Adv Technol.* 2022;33(4):1057-1068. doi:10.1002/pat.5578